

The Investigation of Equivalent Harmonic Impedances of VSC-Based HVDC Systems

Phuchuy Nguyen and Minxiao Han

School of Electrical Engineering, North China Electric Power University, Beijing 102206, P.R. China

Email: huynp@epu.edu.vn, hanminxiao@163.cn

Abstract—In a PWM-based low level voltage source converter (VSC), the harmonic level is significant that filters should be required on the both sides of the converter. The converter will have harmonic impedances as seen from the both sides, and it matters to assess these impedances to calculate their impact on filters and the network also. In this paper, the equivalent harmonic impedances on both ac- and dc-sides of VSC are calculated based on the ac/dc harmonic interaction with any switching components. The effect of cross-interaction between switching components on the harmonic impedance is also investigated. Moreover, the resonance analysis is performed on the both ac-side and dc-side of a VSC-based HVDC system. Although the VSC dc-side harmonic impedance is very large, the resonances may occur due to the existence of dc capacitors and dc cables. On the ac-side, the resonances may occur at the output terminal of the converter and interact with the dc-side circuit, causing harmonic amplification.

Index Terms—VSC, VSC-based HVDC, resonance, harmonic impedance

I. INTRODUCTION

The introduction of Voltage-Sourced Converter (VSC)-based HVDC to power system offers the potential to improve control of power flow and enhance system stability. However, VSC-based HVDC producing harmonics on the both ac-side and dc-side is inherent by the VSC itself, and will interact with harmonic distortions already existed in the system. The harmonics of VSC are directly associated with the type of VSC technologies, modulation techniques and the switching frequency [1].

Harmonics are transferred between the two sides of the VSC and may interact with the ac system leading to disadvantage effects. A practical case in [2] shows that harmonic instability may occur if there is an unbalanced second harmonic generated by a nearby saturated transformer on the ac-side of VSC. Based on analyzing basic current and voltage equations of (Current Source Converter) CSC and VSC, the authors in [3] establish simple rules of harmonic transfer through converters by using switching functions represented in space vector form. For resonance and filter studies, the converter's harmonic impedances are important. The ac- and dc-side impedances of conventional line-commutated HVDC converters were calculated by applying the harmonic

transfer rules [4]. In the case of VSC, the dc equivalent impedance of VSC is formulated in [5] for analyzing non-integral harmonic resonance from the interaction of AC/DC systems. The ac equivalent impedance of VSC is formulated in [6] also based on the harmonic transfer through VSC. However, all the authors just investigated the interaction of the fundamental switching component only.

Harmonic transfer rules of VSC are valid for both voltage harmonics and current harmonics. Based on the rules, this paper formulated the ac- and dc-side harmonic impedances of the VSC by using the switching functions represented in space vector form. The harmonic impedances derived with considering not only the fundamental switching component, but also the high frequency switching ones of the VSC's switching functions. The influences of switching components on these harmonic impedances are dominant if the sequence of interacted harmonic is the same to the sequence of the switching components. Moreover, the cross-interaction between switching components was also investigated. Consequently, the dc- and ac-side equivalent harmonic impedances of the VSC in VSC-based HVDC systems were used in the ac- and dc-side to plot driving point impedance curves, giving a clearer view of the harmonic resonance analysis.

II. VSC AC- AND DC-SIDE HARMONIC IMPEDANCES

Harmonic impedance of the VSC responds the relation between voltage and current at different frequencies. For simplicity, assuming that the VSC analyzed in this case is symmetric. In the time domain, the relation between these two quantities can be expressed as (1) [7].

$$\begin{cases} \bar{u}_v(t) = \bar{K}(t) \cdot u_d(t) / 2 \\ i_d(t) = \frac{3}{4} \text{Re} \left[\left[\bar{K}(t) \right]^* \bar{i}_v(t) \right] \end{cases} \quad (1)$$

where

$\bar{u}_v(t), \bar{i}_v(t)$: Space vector of ac-side voltage and current.

$u_d(t), i_d(t)$: DC-Side voltage and current.

$\bar{K}(t)$: The space vector of three sinusoidal switching functions.

The switching function comprises the fundamental frequency component called frequency switching component, and high-frequency ones called high-order

switching components. The harmonic interaction rules between two sides of the VSC with the fundamental switching component were introduced in [7]. For individual N^{th} switching component, the space vector can be expressed as:

$$\bar{K}(t) = \hat{K}_N e^{j\omega_N t} \quad (2)$$

Generally, a background harmonic of ω on the ac-side will produce only harmonic of $\omega - \omega_N$ on the dc-side; while a background harmonic of ω on the dc-side will transfer to the ac-side and induce two harmonic of $\omega_N + \omega$ and $\omega_N - \omega$. The effect of these additional harmonics should be taken into account in the calculation process of equivalent harmonic impedances.

For convenience, a simple equivalent circuit in Fig. 1 is used for equivalent harmonic impedance calculation on the both sides of the VSC, with Z_{AC} and Z_{DC} respectively is the VSC ac- and dc-side harmonic impedance. The impedances of the ac- and dc-circuit are composed of the equivalent impedances of all ac- and dc-side components seen from the converter's ac- and dc-terminals, respectively.

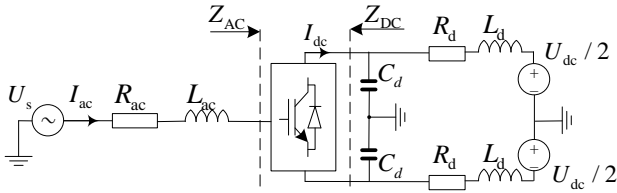


Figure 1. Equivalent circuit diagram for harmonic impedance calculation

A. VSC AC-Side Harmonic Impedance

In this section, the ac-side harmonic current with the frequency of ω is either positive-sequence or negative-sequence. If the positive-sequence harmonic current is $\bar{i}_V^+(t) = I_m e^{j[\omega t + \beta]}$, the corresponding dc-side current, and therefore, the dc-side voltage is

$$u_{dc}^+(t) = \frac{i_{dc}^+(t)}{Y_{dc}^+} = \frac{3\hat{K}_N}{4} \frac{I_m}{Y_{dc}^+} \cos[(\omega - \omega_N)t + \beta] \quad (7)$$

This dc-side voltage will be fed back to the ac-side and induces a positive voltage and a negative voltage mentioned in the previous section. The ac-side induced negative voltage contributes to the dc-side current again; therefore, the admittance in (7) will be the sum of the dc circuit admittance and the negative admittance part in (6) with $\omega - \omega_N$ is changed to $\omega - 2\omega_N$.

$$Y_{dc}^+ = \frac{1}{Z_{dc}(\omega - \omega_N)} + \frac{3\hat{K}_N^2}{16Z_{ac}^-(\omega - 2\omega_N)} \quad (8)$$

The ac-side positive voltage caused by the dc-side voltage in (7) is

$$\bar{u}_V^+(t) = \frac{3\hat{K}_N}{16} \frac{I_m}{Y_{dc}^+} e^{j[\omega t + \beta]} \quad (9)$$

The VSC positive harmonic admittance on the ac-side is now calculated as

$$Y_{AC}^+(\omega) = \frac{\bar{i}_V^+(\omega)}{\bar{u}_V^+(\omega)} = \frac{16}{3\hat{K}_N^2} \left[\frac{1}{Z_{dc}(\omega - \omega_N)} + \frac{3\hat{K}_N^2}{16Z_{ac}^-(\omega - 2\omega_N)} \right] \quad (10)$$

The negative harmonic admittance, when ac-side exists a negative-sequence background harmonic, is similarly established and can be expressed as (11).

$$Y_{AC}^-(\omega) = \frac{16}{3\hat{K}_N^2} \left[\frac{1}{Z_{dc}(\omega + \omega_N)} + \frac{3\hat{K}_N^2}{16Z_{ac}^+(\omega + 2\omega_N)} \right] \quad (11)$$

Equation (10) and (11) are the inversion of the VSC ac-side positive and negative harmonic impedance, respectively.

B. Cross-Interaction between Switching Components

Beside the fundamental switching component, the high-order switching ones of VSC's switching function also contribute to produce additional harmonics on both ac- and dc-side. In this case, we consider the contribution of the fundamental and a high-order switching component and the cross-interaction between them in calculating harmonic impedance. The switching function in (2) is now can be expressed as

$$\bar{K}(t) = \hat{K}_1 e^{j\omega_1 t} + \hat{K}_N e^{j\omega_N t} \quad (12)$$

where $\hat{K}_1 = M$ is the modulation index.

The harmonic impedances on the both sides of the VSC could be derived by using the similar procedure in the section 2.1 and 2.2. The total VSC dc-side harmonic impedance is

$$Y_{DC}(\omega) = \frac{3(\hat{K}_1^2 + 3\hat{K}_1\hat{K}_N)}{16} \left[\frac{1}{Z_{ac}^+(\omega + \omega_1)} + \frac{1}{Z_{ac}^-(\omega - \omega_1)} \right] + \frac{3(\hat{K}_N^2 + 3\hat{K}_1\hat{K}_N)}{16} \left[\frac{1}{Z_{ac}^+(\omega + \omega_N)} + \frac{1}{Z_{ac}^-(\omega_N - \omega)} \right] \quad (13)$$

The total VSC ac-side harmonic impedance in this case can be calculated by (14).

$$Z_{AC}^s(\omega) = \frac{3}{16} \left[\frac{\hat{K}_1^2 + \hat{K}_1\hat{K}_N}{Y_{dc1}^s} + \frac{\hat{K}_N^2 + \hat{K}_1\hat{K}_N}{Y_{dcN}^s} \right] \quad (14)$$

where $s=1$ for positive harmonic impedance, and $s=-1$ for negative one; Y_{dc1}^s and Y_{dcN}^s are defined as (15).

$$\left\{ \begin{array}{l} Y_{dc1}^s = \frac{1}{Z_{dc}(\omega - s\omega_1)} + \frac{3}{16} \left[\frac{\hat{K}_N^2 + \hat{K}_1\hat{K}_N}{Z_{ac}(\omega - s\omega_1 - s\omega_N)} + \frac{\hat{K}_1^2 + \hat{K}_1\hat{K}_N}{Z_{ac}(\omega - s2\omega_1)} \right] \\ Y_{dcN}^s = \frac{1}{Z_{dc}(\omega - s\omega_N)} + \frac{3}{16} \left[\frac{\hat{K}_1^2 + \hat{K}_1\hat{K}_N}{Z_{ac}(\omega - s\omega_1 - s\omega_N)} + \frac{\hat{K}_N^2 + \hat{K}_1\hat{K}_N}{Z_{ac}(\omega - s2\omega_N)} \right] \end{array} \right. \quad (15)$$

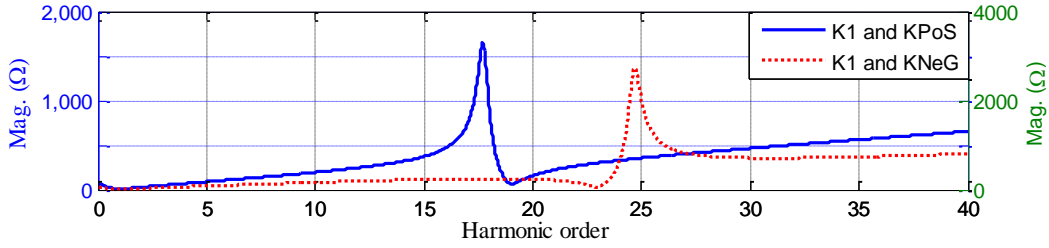


Figure 2. DC-side harmonic impedance with cross-interaction

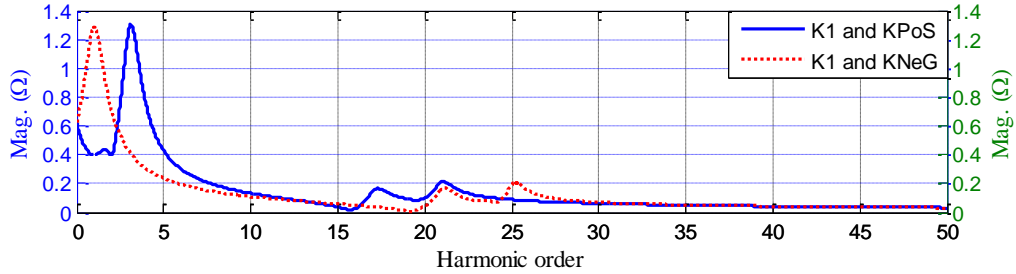


Figure 3. AC-side harmonic impedance with cross-interaction

Fig. 2 and Fig. 3 show the harmonic impedance characteristics of the circuit in Fig. 1 with parameters as: $R_{ac} = 1\Omega$, $L_{ac}=11.7\text{mH}$, $C_d = 500\text{ F}$, $R_d = 2\Omega$, $L_d = 5\text{mH}$; VSC: Modulation index $M = 0.8$, switching frequency $f_c = 1050\text{Hz}$.

Fig. 2 illustrates the VSC dc-side harmonic impedance characteristic in considering the cross-interaction between the fundamental switching component (K1) and high-order positive (KPoS) and negative (KNeG) switching components. Clearly, the parallel resonance points tend to appear at the frequency lower than the frequency of KPoS and higher than the frequency of the KNeG.

Fig. 3 illustrates the VSC ac-side harmonic impedance under the cross-interaction between K1 and KPoS, and between K1 and KNeG, for both cases of positive and negative sequence background harmonic, respectively. The harmonic impedance characteristics have small changes with two parallel resonance points closed to the switching frequency.

III. RESONANCE ANALYSIS OF VSC-BASED HVDC SYSTEM

A. VSC-Based HVDC System Model

The VSC-based HVDC system is a point-to-point scheme which consists of two VSC stations interconnected by $\pm 300\text{kV}$ dc cables and transfers power of 600MW from 330kV ac system ($I_{scmax1} = 50\text{kA}$) to 230kV ac system ($I_{scmax2} = 40\text{kA}$). Fig. 4 represents the main components of one half of the system with filters are installed on the both sides of the converter station. The equivalent impedance circuit is shown in Fig. 5.

In Fig. 5(a), Z_{AC1} is the VSC1 ac-side harmonic impedance; Z_{S1} , Z_{T1} , Z_{R1} and Z_{F1} are equivalent impedances of ac system 1, converter transformer, converter reactor and filter respectively; PCC1 is the Point of Common Connection and A1 is the VSC1's

output terminal. In Fig. 5(b), Z_{DC1} and Z_{DC2} are respectively the VSC1 and VSC2 dc-side harmonic impedances; DC-link equivalent circuit includes dc smoothing reactors (Z_{L1} , Z_{L2}), dc-filters and dc capacitors (Z_{CF1} , Z_{CF2}), and the dc-cables. The dc-cables are modeled as PI model, and their shunt capacitances are at the proportional rate along the cable length that exploited to reduce the size of the dc capacitors [8]. The parameters of components are: dc capacitors $C_d = 30\text{F}$; dc-cables: $R_c = 13.9\text{m}\Omega/\text{km}$, $L_c=0.159\text{mH}/\text{km}$, $C_c = 0.231\text{F}/\text{km}$, $L_{cab} = 850\text{km}$; reactor $X_R=0.15\text{p.u.}$

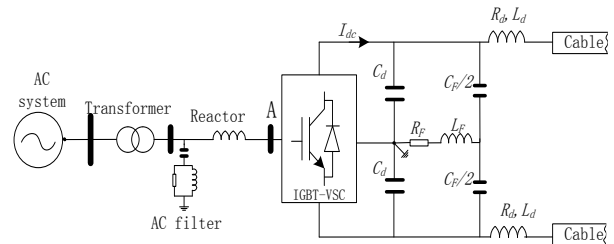


Figure 4. Schematic diagram of one half of the studied VSC-HVDC system

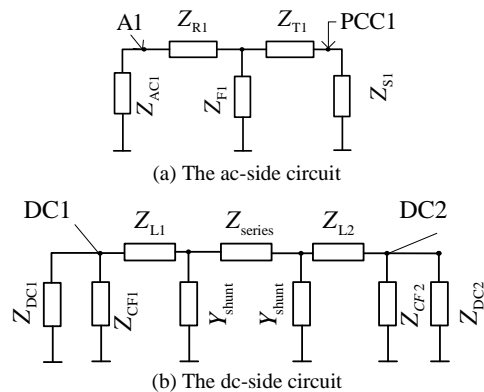


Figure 5. Impedance model for resonance analysis of the VSC-based HVDC system

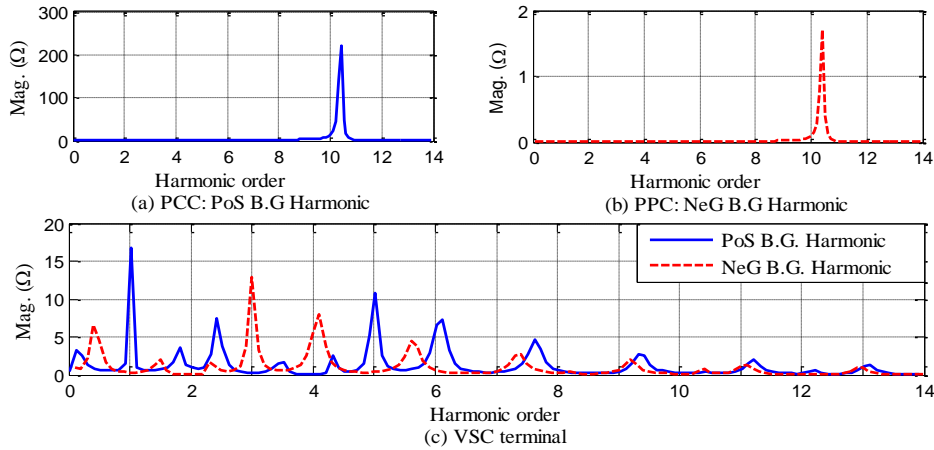


Figure 6. Driving point impedance seen from different points of the ac-side circuit

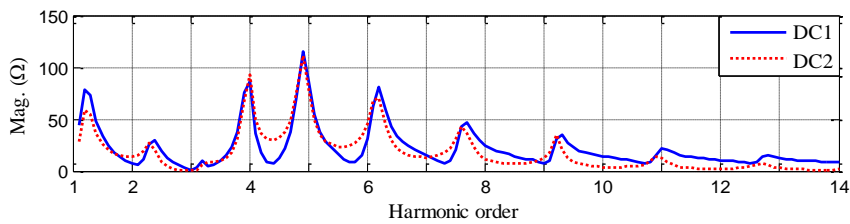


Figure 7. DC-Side driving point impedance seen from VSC1 (blue) and VSC2 (red) dc-terminals

B. Result Analysis

Fig. 6 shows the driving point impedance as seen from the Point of Common Coupling (PCC) and the VSC’s output terminal (A point) in both cases of PoS and NeG background harmonics. At the PCC point (Fig. 6(a) and Fig. 6(b)), there exists only one resonant point close to the tenth harmonic in the both cases, but the magnitudes are different. At the ac terminal of the VSC (Fig. 6(c)), a series and resonance points appear with parallel resonances at the NeG 3rd harmonic and PoS 5th harmonic.

Fig. 7 shows the driving point impedances seen from the dc terminal of VSC1 (DC1), and the dc terminal of VSC2 (DC2) referred to the DC1 point. The impedance-frequency responding curves have no change in shape with parallel resonant points appear at the 4th harmonics, and close to the 5th and 6th harmonics. Because of the 3rd harmonic filter, the circuit has a series resonance at the 3rd harmonic.

In Fig. 7, the 4th harmonic voltage at the dc terminal of VSC1 will increase largely with a small 4th harmonic current injected in. This 4th harmonic transferred to the ac-side and causing parallel resonance points with the PoS 5th harmonic and NeG 3rd harmonic (see Fig. 6(c)), this is called composite resonance between ac- and dc-side, so that the feedback to the dc-side is insignificant. It should be noted that for a VSC, the feed back from the dc-side to the ac-side is significant with parallel resonances on the dc-side; however, the feed back from the ac-side to the dc-side is significant with a series resonances.

IV. CONCLUSION

The harmonic impedances on the both sides of VSC were calculated based on the switching technique and

harmonic interaction characteristic of the converter. With different switching components, the contributions on harmonic impedance calculation are different. The fundamental switching component is the largest and therefore, contributes the most to equivalent harmonic impedances in both cases of positive and negative sequence background harmonics. For the high frequency switching components, they contribute dominantly in cross-interaction with the fundamental one if they have same sequences with the background harmonics.

The VSC ac- and dc-side harmonic impedances are beneficial to resonance analysis and filter designs in the VSC-based HVDC system. The impedance-frequency responses give a visual view at which frequency resonance points appear, which gives the aid of proposing effective relevant mitigation methods, minimizing the site measurements in harmonic investigations.

ACKNOWLEDGMENT

This work was supported by State Grid Cooperation of China, Major Projects on Planning and Operation Control of Large Scale Grid SGCC-MPLG019-2012, National Science Foundation of China: 51177044.

REFERENCES

- [1] N. Flourentzou, V. G. Agelidis, and G. D. Demetriades, “VSC-Based HVDC power transmission systems: An overview,” *IEEE Transactions on Power Electronics*, vol. 24, pp. 592-602, 2009.
- [2] A. E. Hammad, “Analysis of second harmonic instability for the Chateauguay HVDC/VSC scheme,” *IEEE Trans. Power Delivery* vol. 7, NO. 1, pp. 410-415, Jan. 1992.
- [3] J. Ying and A. Ekstrom, “General analysis of harmonic transfer through converters,” *IEEE Transactions on Power Electronics*, vol. 12, pp. 287-293, 1997.

- [4] P. Riedel, "Harmonic voltage and current transfer, and AC- and DC-side impedances of HVDC converters," *IEEE Transactions on Power Delivery*, vol. 20, pp. 2095-2099, 2005.
- [5] L. Tang and O. Boon-Teck, "Converter nonintegral harmonics from AC network resonating with DC network," in *Proc. IEEE 36th Industrial Application Society Annual Conference*, 2001, vol. 4, pp. 2186-2192.
- [6] G. Yang, *VSC-Based HVDC Transmission System Technology (in Chinese)*, Beijing, China: China Electric Power Press, 2009, pp. 172-177.
- [7] P. Nguyen and M. Han, "Study on harmonic propagation of VSC-based HVDC systems," in *Proc. PowerCon 2014*, Chengdu, China, 2014.
- [8] C. Chang Hsin and R. Bucknall, "Analysis of harmonics in Subsea power transmission cables used in VSC-HVDC transmission systems operating under steady-state conditions," *IEEE Transactions on Power Delivery*, vol. 22, pp. 2489-2497, 2007.



Phuchuy Nguyen received his B.Sc and M.Sc degree from Hanoi University of Science and Technology (HUST), Viet Nam in 2003 and 2010 respectively. Now he is a Ph.D. student in the Electric Power System and Its Automation at North China Electric Power University (NCEPU), Beijing, China. The main research interest is in the field of flexible HVDC transmission systems and power quality.

Minxiao Han was born in Shannxi, China, in 1963. He received his B.Sc. from Xi'an Jiaotong University in 1984, M.Sc. and Ph.D. from North China Electric Power University (NCEPU) in 1987 and 1995 respectively. He was a visiting research fellow in Queen's University of Belfast, U.K. and post-doctoral research fellow with Kobe University, Japan. He is active in professional society activities and international cooperation relating with the field of application of power electronics in power system including HVDC & FACTS, power quality and the integration of renewable generation in power network.